VOL. 6, NO. 2 HVAC&R RESEARCH APRIL 2000

A Damper Control System for Preventing Reverse Airflow Through the Exhaust Air Damper of Variable-Air-Volume Air-Handling Units

John E. Seem, Ph.D.
Member ASHRAE

John M. House, Ph.D.
Associate Member ASHRAE

George E. Kelly, Ph.D.
Member ASHRAE

Curtis J. Klaassen, P.E.
Member ASHRAE

Traditional air-handling unit (AHU) control systems link the position of the exhaust, recirculation, and outdoor air dampers. Laboratory tests of a variable-air-volume AHU using the traditional damper control approach revealed that outdoor air could enter the AHU through the exhaust air damper. This can negatively impact indoor air quality. This paper examines the conditions that lead to this phenomenon and presents a new control system that can help alleviate the problem. The new control system links only the position of the exhaust and recirculation air dampers. During occupied times, the outdoor air damper is fully open.

Simulation results are presented that demonstrate that the new damper control system prevents air from entering the AHU through the exhaust air outlet for all but extreme conditions that are described in the paper. Laboratory and field test results are presented that demonstrate that the new control system prevents air from entering the AHU through the exhaust air outlet for the same conditions that cause significant reverse airflow for the traditional control system. Furthermore, reverse airflow was not observed for any of the conditions examined in the laboratory and field tests when the new control system was used.

INTRODUCTION

The primary function of an air-handling unit (AHU) is to provide conditioned air to occupied areas of a building. An AHU typically has dampers that are used to control the amount of outdoor air that enters the system, the amount of air exhausted from the system, and the amount of return air from the building that is recirculated through the system. Damper control is primarily influenced by two factors, namely, the need to provide sufficient outdoor air to meet indoor air quality (IAQ) standards, and a desire to conserve energy by limiting heating and cooling in the AHU coils. AHUs are designed with the intent that outdoor air enters the system only through the outdoor air duct and dampers. However, under certain conditions air can also enter an AHU through the exhaust air damper. This phenomenon has been observed in laboratory tests of a variable-air-volume (VAV) AHU that utilizes a volume matching control strategy to control building pressurization and, indirectly, the flow of outdoor air into the AHU.

Why is this problem of interest? IAQ could be jeopardized if the exhaust air damper is located near a truck dock, garbage dumpster, or other pollution/odor source. In addition, in some AHUs special filters and/or preheat coils are placed in the outdoor air duct. Air entering the AHU

John E. Seem is a principal research engineer at Johnson Controls, Inc., Milwaukee, WI. **John M. House** is a mechanical engineer and **George E. Kelly** is the Chief of the Building Environment Division, Building and Fire Research Laboratory, National Institute of Standards and Technology, Gaithersburg, MD. **Curtis J. Klaassen** is the manager of the Iowa Energy Center Energy Resource Station, Ankeny, IA.

through the exhaust air damper would bypass these components. Bypassing the special filters could lead to poor IAQ. If the outdoor air temperature is cold enough, the coils could freeze or the freeze protection thermostat could cause the AHU to shut down. Hence, this phenomenon introduces another degree of complexity to the control of VAV AHUs that must be addressed by controls consultants and building operators.

The phenomenon of reverse airflow through the exhaust air damper of VAV AHUs has been noted in the literature (Janu et al. 1995, Elovitz 1995); however, given the potential seriousness of problem, it has not received adequate attention. The objectives of this study are to describe the physical circumstances that tend to produce the reverse airflow phenomenon and to present a control solution that will substantially alleviate the potential for this behavior.

This paper is organized as follows. Typical operating strategies for a VAV AHU are presented first. Next, the equations governing airflow in the AHU are presented and simulation results demonstrating reverse airflow through the exhaust air damper are presented. A new damper control system is then proposed and simulation, laboratory and field results are presented comparing it with the traditional damper control system. Finally, conclusions and recommendations from this study are presented.

THEORETICAL ANALYSIS

System Description

Figure 1 is a schematic diagram of a typical single duct VAV AHU. The AHU consists of variable speed supply and return fans, three dampers for controlling airflow to and from the AHU to the outdoor environment, heating and cooling coils for conditioning the air, a filter for removing airborne particles, various sensors and actuators, and a controller that receives sensor measurements and computes and transmits new control signals. In the discussion that follows, typical operating strategies are described for a VAV AHU that uses volume-matching control of the return fan.

VAV AHUs are typically controlled to maintain a constant set-point temperature at a location in the supply duct downstream of the supply fan. This is achieved by controlling the outdoor air, recirculation air, and exhaust air dampers, and by controlling the flow of hot water and cold water through the heating and cooling coils, respectively. For extreme outdoor air temperatures, the dampers are typically positioned to allow only enough outdoor air to enter the AHU to satisfy minimum ventilation requirements. This type of control can produce significant energy savings.

The supply fan of a VAV AHU is controlled to maintain the static pressure in the supply duct at a constant set-point value. Constant temperature supply air is distributed to various zones (not shown) that may have different loads and/or set-point temperatures. To account for the variability of the conditions in the zones, VAV boxes (not shown) that regulate the amount of air that enters a zone are placed at the end of the supply air ductwork leading to each zone. As a zone load decreases, the corresponding VAV box restricts the flow of air to the zone, thereby increasing the static pressure in the supply duct and causing the supply fan speed to decrease in order to maintain the static pressure set-point condition. If the zone load increases, the VAV box and supply fan respond in the opposite manner.

The return fan of a VAV AHU is typically controlled to maintain a small positive zone pressurization in order to prevent infiltration. One strategy used for this purpose controls the return fan to maintain a constant differential between the supply and return airflow rates. This strategy is known as volume matching control (also known as fan tracking). With this strategy, airflow stations are used to measure the airflow rates in the supply and return air ducts. Because the difference between the supply and return airflow rates (the volume matching differential) must be made up by outdoor air, the volume matching strategy also indirectly controls the amount of out-

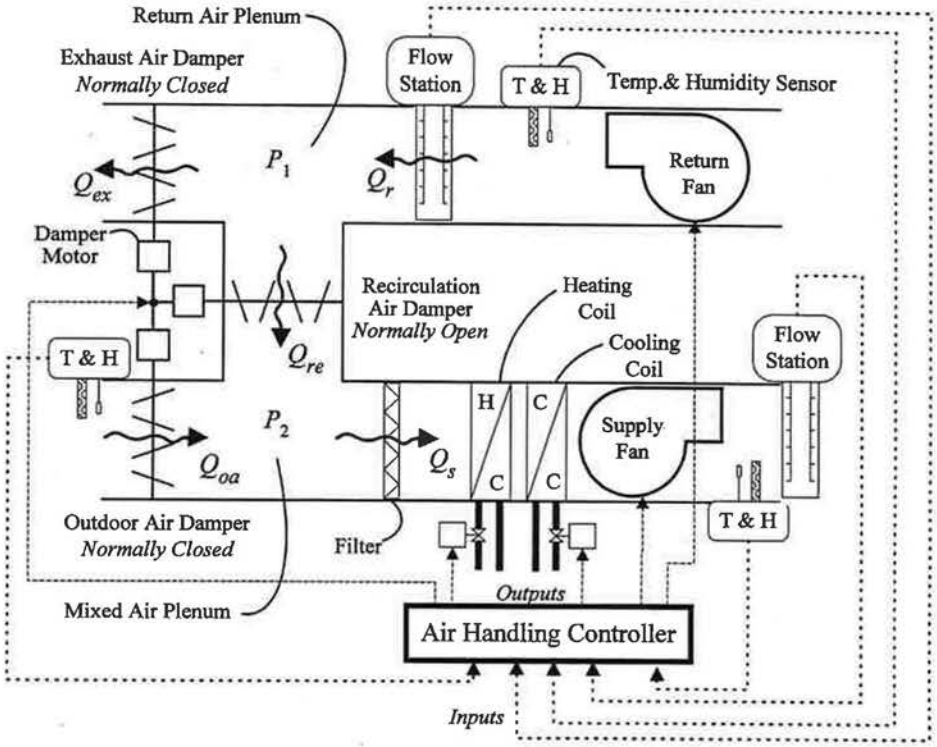

Figure 1. Schematic diagram of single duct variable-air-volume air-handling unit

door air that enters the AHU. Kettler (1995) and Elovitz (1995) provide numerical examples of how the volume matching strategy can lead to large errors in the control of ventilation air and recommend other strategies for controlling ventilation air. Nonetheless, the volume matching strategy is used and is susceptible to the problem described in this paper.

Traditional AHU Damper Control System

Traditional AHU control systems link the position of the outdoor air damper, recirculation air damper, and exhaust air damper. The outdoor and exhaust air dampers are normally closed and the recirculation air damper is normally open. As the outdoor and exhaust air dampers are opened, the recirculation air damper is closed. The dampers may have separate motors as depicted in Figure 1, or they may be mechanically linked and controlled by a single motor. For this traditional system, the equations describing the relationship between damper positions are:

$$\theta_{re} = 1 - \theta_{ex} \tag{1}$$

$$\theta_{out} = 1 - \theta_{re} = \theta_{ex} \tag{2}$$

where θ_{re} is the fraction of fully open position of the recirculation air damper, θ_{ex} is the fraction of fully open position of the exhaust air damper, and θ_{out} is the fraction of fully open position of the outdoor air damper.

Outdoor, recirculation, and exhaust airflow rates are dependent on the characteristics and settings (blade positions) of the dampers, the supply and return airflow rates, and pressures in the return and mixed air plenums as well as the pressure at the inlet to the outdoor air duct and the pressure at the exit to the exhaust air duct. In the next section, the equations governing airflow in VAV AHUs are presented.

Pressure and Airflow Governing Equations

The governing equations for the pressure and airflow conditions in the AHU are derived from the principles of conservation of mass and energy. The density of air is assumed to be constant and the pressures at the inlet of the outdoor air duct and at the exit of the exhaust duct are assumed to be equal to atmospheric pressure (i.e., wind and stack effects are not included in the governing equations). Steady-state conditions are assumed to exist. Neglecting duct leakage, conservation of mass applied at the return air plenum and at the mixed air plenum yields

$$Q_r = Q_{ex} + Q_{re} \tag{3}$$

$$Q_s = Q_{oa} + Q_{re} \tag{4}$$

where Q_r is the return airflow rate, Q_{ex} is the flow rate of air exiting the AHU through the exhaust air damper, Q_{re} is the recirculation airflow rate, Q_s is the supply airflow rate, and Q_{oa} is the flow rate of air entering the AHU through the outdoor air damper. Because of the constant air density assumption, all airflow rates discussed in this paper are volumetric airflow rates.

The energy equation for return air exiting the AHU through the exhaust air damper is (White 1986)

$$\frac{P_1}{\rho} + \frac{V_{ex}^2}{2} = \frac{P_a}{\rho} + (C_{sc} + C_{d,ex} + C_{en})\frac{V_{ex}^2}{2} \tag{5}$$

where C_{sc} is the loss coefficient for a screen that is placed in the exhaust air duct (and outdoor air duct) to prevent birds and other small animals from entering the AHU ductwork, $C_{d,ex}$ is the loss coefficient for the exhaust air damper, C_{en} is the loss coefficient for a sudden enlargement, P_1 is the static pressure in the return air plenum, P_a is atmospheric pressure, V_{ex} is the velocity of air exiting the AHU through the exhaust air damper, and ρ is the air density. The coefficient for a sudden enlargement is used in Equation (5) to account for losses as the air is passing from the exhaust air duct to the outdoor environment.

The energy equation for outdoor air entering the AHU through the exhaust air damper is

$$\frac{P_a}{\rho} = \frac{P_1}{\rho} + \frac{V_{ex}^2}{2} + (C_{co} + C_{d,ex} + C_{sc})\frac{V_{ex}^2}{2} \tag{6}$$

where C_{co} is the loss coefficient for a sudden contraction. In this case the coefficient for a sudden contraction accounts for losses as the air is drawn into the exhaust air duct from the outdoor environment.

The energy equation for outdoor air entering the AHU through the outdoor air damper is

$$\frac{P_a}{\rho} = \frac{P_2}{\rho} + \frac{V_{oa}^2}{2} + (C_{co} + C_{d,oa} + C_{sc})\frac{V_{oa}^2}{2} \tag{7}$$

where $C_{d,oa}$ is the loss coefficient for the outdoor air damper, P_2 is the static pressure in the mixed air plenum, and V_{oa} is the velocity of air entering the AHU through the outdoor air damper.

The energy equation for airflow through the recirculation air damper is

$$\frac{P_1}{\rho} = \frac{P_2}{\rho} + (C_m + C_{d,re})\frac{V_{re}^2}{2} \tag{8}$$

where C_m is a loss coefficient for miscellaneous losses between the return air plenum and the mixed air plenum, $C_{d,re}$ is the loss coefficient for the recirculation air damper, and V_{re} is the velocity of air through the recirculation air duct.

The volumetric airflow rates and air velocities are related by the following expressions:

$$Q_{ex} = V_{ex}A_{ex} \tag{9}$$

$$Q_{oa} = V_{oa}A_{oa} \tag{10}$$

$$Q_{re} = V_{re}A_{re} \tag{11}$$

where A_{ex} is the area of the exhaust air damper where Q_{ex} is measured, A_{oa} is the area of the outdoor air damper where Q_{oa} is measured, and A_{re} is the area of the recirculation air damper where Q_{re} is measured.

To determine the pressures and airflow rates throughout the AHU, it is necessary to specify the loss coefficients in Equations (5) to (8), the damper areas in Equations (9) to (11), and the supply and return airflow rates. Having done this, the governing equations can be solved simultaneously to determine the pressures P_1 and P_2 and the airflow rates Q_{ex}, Q_{oa}, and Q_{re}.

The model described by Equations (3) to (8) yields results that are believed to be representative of actual systems. Because of their custom built nature, each AHU tends to experience unique operating conditions and configurations that influence the airflow characteristics in the system. Thus, the use of the idealized model seems justified for purposes of analyzing the trends in airflow rates and pressures for VAV AHUs.

Simulation Results

Simulations were performed to examine the effect of several design parameters on the airflow and pressure conditions in the AHU. Solutions to the governing equations were obtained using a general purpose equation solver (Klein and Alvardo 1994). A base case simulation was performed to establish representative airflow characteristics and rates for a typical operating condition. The following values were used in the base case simulation:

Q_s = 4.0 m^3/s
$Q_s - Q_r$ = 1.0 m^3/s
P_a = 1 atm
A_{ex} = 2.0 m^2
A_{oa} = 2.5 m^2
A_{re} = 1.0 m^2
ρ = 1.202 kg/m^3
C_{sc} = 0.32 (ASHRAE 1993b)
C_{co} = 0.5 (De Nevers 1977)
C_{en} = 1.0 (De Nevers 1977)
C_m = 1.0

The values of the loss coefficient for a sudden contraction (C_{co}) and the loss coefficient for a screen (C_{sc}) listed above were used for both the exhaust and the outdoor air ducts. Standard ASHRAE sizing practices (ASHRAE 1993b) were used to determine representative values for the base case conditions. Nonlinear functions fit to ASHRAE loss coefficient data (1989, 1993a) were used to estimate values of $C_{d,ex}$, $C_{d,oa}$ and $C_{d,re}$ as a function of damper position.

Figures 2 to 4 present simulation results of the exhaust airflow rate as a function of the position of the outdoor air damper for various flow conditions. Figure 2 demonstrates the influence of the supply airflow rate on the exhaust airflow rate for base case values of the volume matching differential and recirculation air damper size. Figure 3 shows the influence of the volume matching differential for base case values of the supply airflow rate and recirculation air damper size. Figure 4 shows the influence of the design recirculation air velocity (i.e., recirculation air damper size) for base case values of the supply airflow rate and volume matching differential. Changes to the design recirculation air velocity are achieved by modifying the size of the recirculation air damper in the simulations.

Figure 2 shows that for a supply airflow rate of 5.0 m^3/s, the airflow rate through the exhaust air damper is negative if the outdoor air damper is less than 20% open. This means that outdoor air enters the AHU through the exhaust air damper. As the supply airflow rate decreases (and the volume matching differential is held constant), the exhaust airflow rate remains negative for larger values of the outdoor air damper position. Thus, the reverse airflow phenomenon becomes more evident in a VAV air-handling system at low load conditions when the supply airflow rate is decreased. As the outdoor air damper approaches the closed position, the exhaust airflow rate becomes insensitive to the supply airflow rate.

Ideally the exhaust airflow rate would be zero when the exhaust air damper is fully closed. Because the damper control system links the damper positions, a fully closed exhaust air damper corresponds directly to a fully closed outdoor air damper. To achieve this ideal airflow scenario, the exhaust air damper loss coefficient ($C_{d,ex}$) must approach infinity as the damper approaches

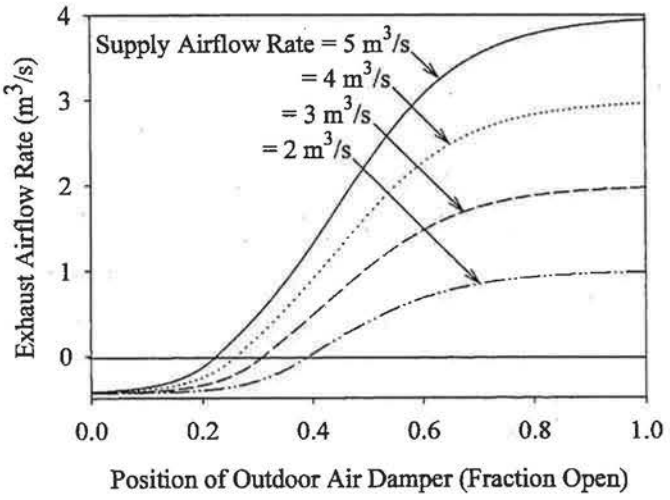

Figure 2. Simulated exhaust airflow rate as a function of outdoor air damper position and supply airflow rate using base case values for all other parameters

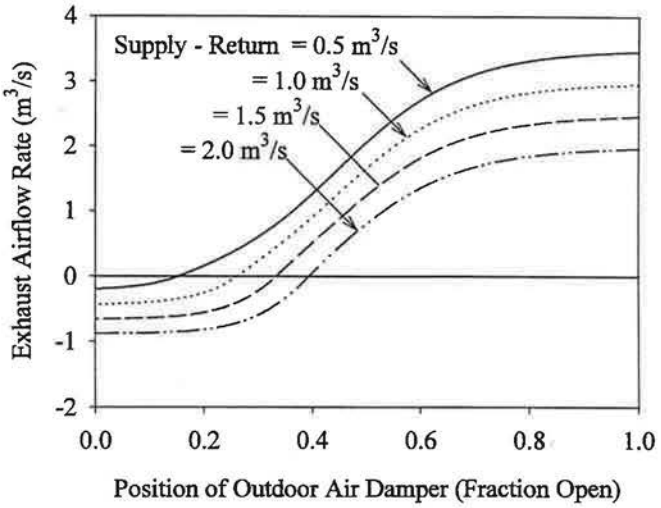

Figure 3. Simulated exhaust airflow rate as a function of outdoor air damper position and volume matching differential using base case values for all other parameters

the fully closed position. In the simulation results, the damper loss coefficients have finite values when the dampers were in the fully closed position.

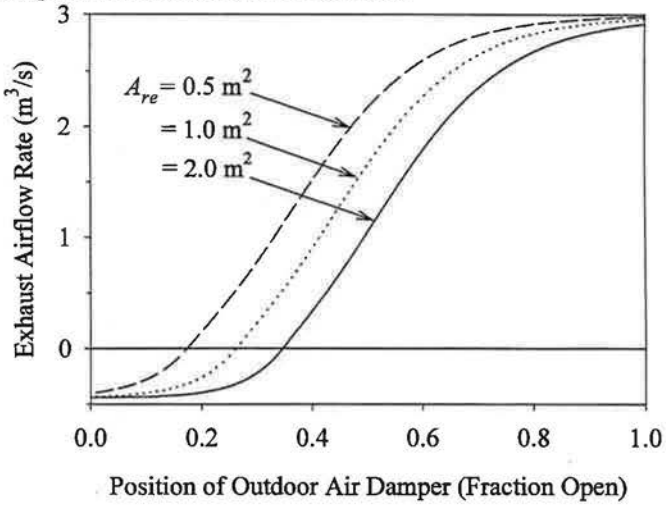

Figure 4. Simulated exhaust airflow rate as a function of outdoor air damper position and design recirculation air velocity using base case values for all other parameters

Figure 3 shows that the exhaust airflow rate is dependent on the volume-matching differential when the outdoor air damper is closed. Larger airflow rate differences between the supply and return air ducts lead to lower return airflow rates (assuming all other parameters are fixed) and

lower return fan speeds. Consequently, the pressure in the return air plenum is lower and larger negative exhaust airflow rates result.

Figure 4 shows that as the design recirculation air velocity decreases (recirculation damper size increases), the amount of air exhausted also decreases for a given supply airflow rate, volume matching differential, and damper position. Larger design recirculation air velocities produce larger pressure drops across the recirculation air dampers for a given damper loss coefficient. This has the same effect as increasing the loss coefficient of the recirculation air damper while maintaining the recirculation air velocity at a constant value, namely, it increases the flow resistance along the path of air entering the AHU through the exhaust air damper, thereby reducing the range of conditions over which the problem occurs.

Figure 4 also shows that in the limit as the outdoor air damper approaches a fully open or fully closed position, the curves collapse upon one another. When the outdoor air damper is nearly fully open, the recirculation air damper is nearly fully closed. In this position, even at lower velocities, the flow resistance associated with the recirculation air damper is sufficiently large to almost completely stop the flow of air through the recirculation air damper (if $Q_{ex} = Q_r = 3.0$ m^3/s, then $Q_{re} = 0$). When the outdoor air damper is nearly fully closed, the recirculation air damper is nearly fully open. In this position the resistance associated with the recirculation air damper is essentially negligible, the flow conditions are insensitive to the design recirculation air velocity and there is reverse flow through the exhaust air damper.

Figure 5 shows the ratio of the outdoor airflow rate (sum of airflow rates entering the AHU through the outdoor and exhaust air dampers) to the supply airflow rate as a function of the outdoor air damper position for various supply airflow rates. Results in Figure 5 can be obtained by applying conservation of mass relations to the results in Figure 2. Similar results were obtained using Figures 3 and 4, but are not presented here.

For a supply airflow rate of 5.0 m^3/s, Figure 5 shows that the outdoor airflow ratio is constant when the outdoor air damper position is less than approximately 20% open. As the supply airflow rate decreases, the minimum value of the outdoor airflow ratio increases. The outdoor air

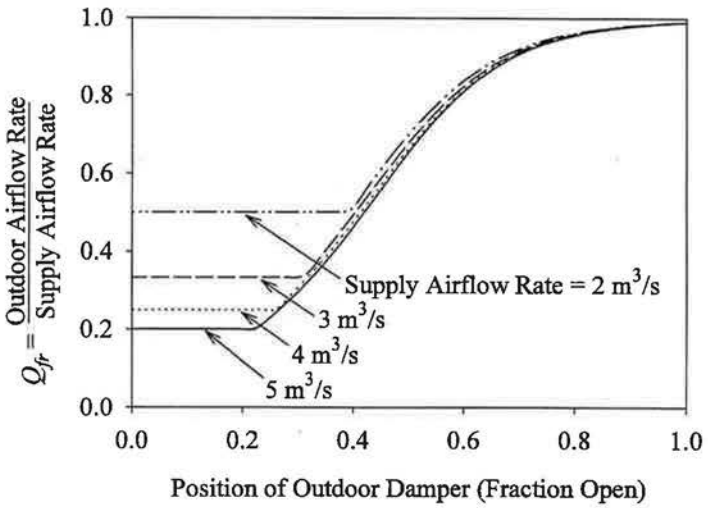

Figure 5. Simulated outdoor airflow ratio as a function of outdoor air damper position and supply airflow rate using base case values for all other parameters

damper position corresponding to the point where the transition to a constant outdoor airflow ratio occurs will be referred to as the threshold position and the corresponding outdoor airflow ratio will be referred to as the threshold outdoor airflow ratio. The threshold outdoor airflow ratio is determined from the supply airflow rate and the volume matching differential. For instance, when Q_s = 2.0 m^3/s and Q_r = 1.0 m^3/s, the makeup airflow rate (outdoor airflow rate minus the exhaust airflow rate) must equal 1.0 m^3/s. The threshold outdoor airflow ratio of 0.5 is reached when the outdoor air damper angle is equal to 0.4. As the outdoor air damper angle is closed further, air is drawn in through the exhaust air damper to provide the necessary makeup air; however, the total amount of outdoor air remains equal to 1.0 m^3/s.

The existence of a threshold outdoor airflow ratio can be shown using the following expression:

$$Q_{fr} = Q_{oa} + \frac{|Q_{ex}| - Q_{ex}}{2} \tag{12}$$

where Q_{fr} is the total outdoor airflow rate accounting for air entering through the outdoor and exhaust air dampers. Equation (12) can be rewritten using Equations (3) and (4) to obtain

$$\frac{Q_{fr}}{Q_s} = 1 - \frac{Q_{re}}{Q_s} + \frac{\left|\frac{Q_r}{Q_s} - \frac{Q_{re}}{Q_s}\right| - \left(\frac{Q_r}{Q_s} - \frac{Q_{re}}{Q_s}\right)}{2} \tag{13}$$

If Q_r/Q_s is constant and Q_{re}/Q_s is gradually increased (implying that the outdoor air damper is gradually closed), Equation (13) yields a constant value of Q_{fr}/Q_s for values of Q_{re}/Q_s greater than or equal to Q_r/Q_s.

There are two main implications of the behavior seen in Figure 5. First, when the outdoor air damper position is less than the threshold position, the amount of outdoor air introduced to the AHU (through both the outdoor and exhaust air ducts) cannot be controlled. Second, as the dampers are modulated to provide free cooling, the system gain (ratio of the change in the temperature at the exit of the mixed air plenum to the change in the damper control signal) becomes zero when the outdoor air damper position is less than the threshold position. If the system gain determined when the outdoor air damper position is less than the threshold position is used to tune the damper controller, the controller may be far too aggressive when the outdoor air damper position is greater than the threshold position. Hence, when tuning the system, the outdoor air damper should be stroked from 40 to 60% open to avoid this potential problem.

NEW AIR-HANDLING UNIT DAMPER CONTROL SYSTEM

The new AHU damper control system links the position of only the exhaust air damper and the recirculation air damper using the relationship in Equation 1. During occupied times, the outdoor air damper remains 100% open, i.e., $\theta_{out} = 1$.

Simulation Results

Simulations were performed to compare the traditional and new control systems. Figure 6 shows the flow rate of air through the exhaust air damper for the traditional and new control systems. Negative values of the exhaust airflow rate indicate that air is entering the AHU through the exhaust air damper. For the traditional control system, outdoor air enters the AHU through the exhaust air damper when it is less than 30% open. For the new control system, outside air does not enter the AHU through the exhaust air damper. By opening the outdoor air damper, the flow resistance through the outdoor air duct is reduced and the pressure in the mixing plenum is increased. This increases the pressure in the return plenum to the point where it is greater than

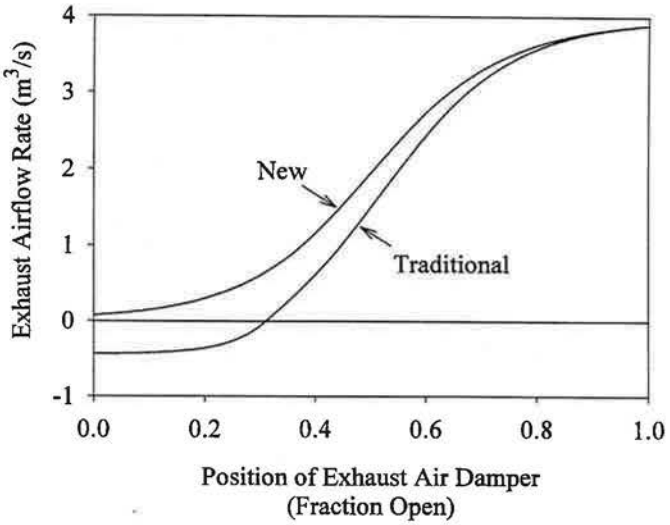

Figure 6. Simulation results comparing traditional and new damper control systems

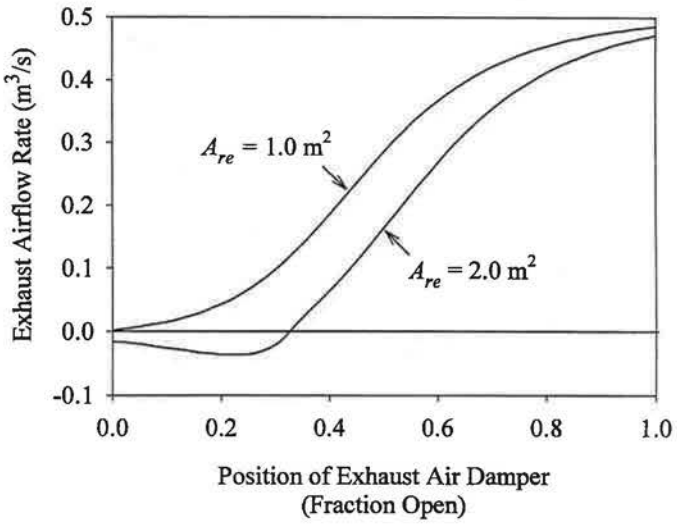

Figure 7. Simulation results for the new control system demonstrating case where new control system fails to prevent reverse airflow through the exhaust damper

atmospheric pressure, thus preventing the reverse airflow phenomenon. Note that as the exhaust air damper approaches the fully open position, the curves in Figure 6 converge. This desirable (albeit expected) result is seen in all ensuing comparisons of the two control systems.

Figure 7 demonstrates a case in which the new control system fails to prevent the reverse airflow problem. Both curves in Figure 7 represent results obtained using the new control system. The curve labeled $A_{re} = 2.0$ m^2 shows that the new control system is unable to prevent the reverse airflow phenomenon when the exhaust air damper is nearly fully closed. The second curve shows that by reducing the area of the recirculation air damper (by disabling and closing one or more blades), air is prevented from entering the AHU through the exhaust air damper. An alternative to reducing the area of the recirculation air damper is to limit its maximum open position.

The results in Figure 7 are presented to demonstrate that the new control system does not eliminate the possibility of outdoor air entering the AHU through the exhaust air damper, it simply reduces the likelihood of occurrence of the phenomenon. In addition, for those cases where reverse airflow through the exhaust air damper does occur with the new control system, the amount of reverse airflow and the range of damper positions over which the phenomenon occurs will be at least as great for the traditional control system. Under extreme conditions, it may be necessary to use the new control system and modify the flow resistance through the recirculation air damper to alleviate the problem.

Laboratory Results

A laboratory VAV AHU was used to validate the findings from the simulations. No attempt was made to measure the actual damper loss coefficients or other loss coefficients for the laboratory AHU. In addition, the sizing of the components of laboratory AHU do not necessarily follow ASHRAE guidelines. Thus, only consistency in trends between the simulation and laboratory results and differences between the new and traditional control systems were validated with the laboratory AHU. Airflow measurements were obtained using airflow stations and differential pressure transducers. The airflow stations yield an average velocity pressure for a cross section of the duct. The differential pressure transducers are accurate to ± 0.05% of the reading + 0.001% of full scale (Datametrics, Inc. 1980).

The exhaust airflow rates for the traditional and new control systems are plotted in Figure 8 as a function of the normalized control signal to the exhaust air damper, where normalized control signals of 0 and 1 indicate that the damper is commanded to the fully closed and fully open positions, respectively. The dashed (traditional) and solid (new) curves in Figure 8 are fourth order

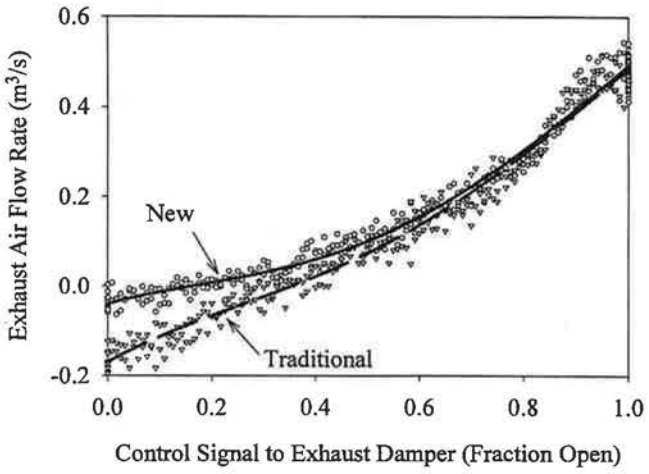

Figure 8. Laboratory results for traditional and new control systems

polynomials that were fit to the data using least-squares regression. For the laboratory results, the supply airflow rate was nearly constant and approximately equal to Q_s = 1.38 m^3/s. The return fan was controlled to maintain the flow difference between the supply and return air ducts at 0.57 m^3/s.

The curves in Figure 8 are very similar to the simulation results presented in Figure 6. Although the data for the new control system indicate that airflow through the exhaust air damper becomes negative as the exhaust air damper is closed, no evidence of reverse airflow through the exhaust air damper was observed when smoke tests were performed. The smoke tests consisted of holding a smoke generator near the exhaust air outlet and observing whether the smoke was blown away from the outlet or drawn into the outlet as the dampers were stroked from fully open to fully closed. Smoke tests confirmed that air is drawn into the AHU when the traditional control system is used and the exhaust air damper approaches the fully closed position. It is possible that the small negative airflow rates seen in Figure 8 for the new control system are attributable to difficulties associated with obtaining accurate airflow measurements.

Field Results

Field tests were performed with both control systems for an AHU at the Iowa Energy Center Energy Resource Station (ERS) located near Des Moines, Iowa. The AHU at the ERS has opposed blade dampers, each with a separate actuator. Commercially available airflow measuring stations that use thermal sensing technology were used to measure the supply, return, and outdoor airflow rates. The rated accuracy of the flow measuring stations is ± 2% of reading.

A custom-made airflow direction indicator was installed in the exhaust air duct. The airflow direction indicator consisted of a light foamboard panel fastened to a pivot rod and pointer. The pivot rod was suspended from the sides of a horizontal section of the exhaust duct. The foamboard panel was nearly the same size as the duct cross sectional area, making it very sensitive to airflow direction and velocity. At no flow or neutral flow conditions the foamboard panel would hang vertically in the duct and the pointer would point down. As the exhaust airflow changed, the panel would rotate on the pivot rod corresponding to the direction and relative magnitude of exhaust airflow. This device made it very easy to determine the direction of airflow in the exhaust air duct.

Two sets of data were collected at the field site. In the first test, the supply airflow rate varied from 1.33 m^3/s to 1.57 m^3/s. In the second test, the supply airflow rate varied from 0.85 m^3/s to 0.96 m^3/s. For each test, the return fan was controlled to maintain the flow difference between the supply and return air ducts at 0.28 m^3/s. The measured flow difference varied from approximately 0.17 m^3/s to 0.36 m^3/s.

Exhaust airflow rates for the two test cases are plotted in Figure 9 (first test case) and Figure 10 (second test case). In each figure, the exhaust airflow rate for the traditional and new control systems is plotted as a function of the control signal to the exhaust air damper. The curves in Figures 9 and 10 are sixth order polynomials that were fit to the field data using least-squares regression. Note that the curves in Figures 9 and 10 appear to have the same shape as the curves presented in Figure 6 for the simulation results and Figure 8 for the laboratory results. From Figure 9 it appears that the traditional control system allows reverse airflow and that the new control system prevents reverse airflow. The airflow direction indicator confirmed that when the exhaust air damper is less than 30% open, air is drawn into the AHU with the traditional control system.

The results in Figure 10 indicate that both control systems allow air to enter the AHU through the exhaust air damper, although the problem is much less severe for the new control system than the traditional control system. It is important to note that the airflow direction indicator did indicate reverse airflow with the traditional control system when the exhaust air damper was less than 35% open; however, *no reverse airflow was observed with the new control system.* As

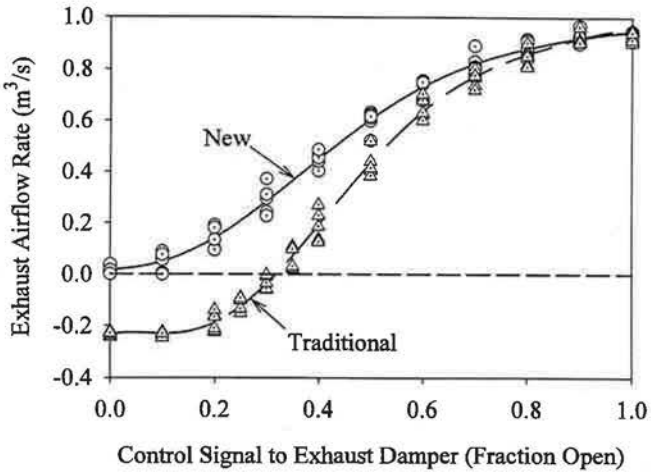

Figure 9. Field results for traditional and new control systems
(Q_s = 1.33 m^3/s to 1.57 m^3/s and $Q_s - Q_r$ = 0.17 m^3/s to 0.36 m^3/s)

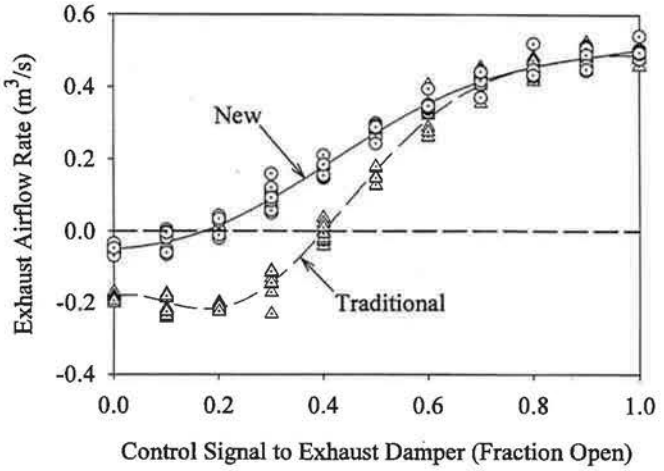

Figure 10. Field results for traditional and new control systems
(Q_s = 0.85 m^3/s to 0.96 m^3/s and $Q_s - Q_r$ = 0.17 m^3/s to 0.36 m^3/s)

speculated for the laboratory results, the small negative airflow rates for the new control system are probably attributed to difficulties obtaining accurate airflow measurements.

CONCLUSIONS

The objectives of this study were to describe the physical circumstances that lead to reverse airflow through the exhaust air damper of VAV AHUs that use volume-matching control, and to present a control solution that will substantially alleviate the potential for this behavior. Simulation, laboratory, and field results presented in this paper demonstrate that air can enter an AHU through the exhaust air damper for a traditional damper control system that links the positions of

the outdoor air damper, exhaust air damper, and recirculation air damper. Simulation results reveal that reverse airflow through the exhaust air damper occurs as the outdoor and exhaust air dampers are closed, and that the phenomenon becomes more pronounced as the volume matching differential becomes a larger percentage of the supply airflow rate. In addition, simulation results demonstrate that increasing the flow resistance through the recirculation air duct helps prevent the reverse airflow problem.

The new control system links only the positions of the exhaust and recirculation air dampers and was developed for AHUs that use a volume matching control strategy for the return fan. For the new control system, the outdoor air damper is fully open during occupied times. Simulation, laboratory, and field results demonstrate that the new control system helps prevent air from entering AHUs through the exhaust air outlet. However, the new control system will not prevent reverse airflow for poorly designed AHUs operating under extreme conditions. For situations in which reverse airflow occurs using the new control system, the problem will also occur and will be more severe with the traditional control system. The new control system is easy to implement and will reduce the range of conditions for which air can be drawn into the AHU through the exhaust air damper.

ACKNOWLEDGMENTS

The authors would like to acknowledge the Office of Building Systems within the U.S. Department of Energy, Office of Building Technology, State and Community Programs for their support of this work. The authors would also like to acknowledge John Webster, Technical Assistant at the Iowa Energy Center Energy Resource Station for his contribution to this study.

NOMENCLATURE

A_{ex} area of exhaust air damper where Q_{ex} is measured
A_{oa} area of outdoor air damper where Q_{oa} is measured
A_{re} area of recirulation air damper where Q_{re} is measured
C_{co} loss coefficient for a sudden contraction
C_{en} loss coefficient for a sudden enlargement
$C_{d,ex}$ loss coefficient for the exhaust air damper
$C_{d,oa}$ loss coefficient for the outdoor air damper
$C_{d,re}$ loss coefficient for recirculation air damper
C_m miscellaneous loss coefficient between return air plenum and mixed air plenum
C_{sc} loss coefficient for a screen
P_1 static pressure in return air plenum
P_2 static pressure in mixed air plenum
P_a atmospheric pressure
Q_r return airflow rate
Q_{ex} airflow rate leaving AHU through exhaust air damper
Q_{fr} total fresh airflow rate accounting for flow into AHU through outdoor air damper and through exhaust air damper
Q_{re} recirculation airflow rate
Q_s supply airflow rate
Q_{oa} airflow rate entering AHU through outdoor air damper
V_{ex} velocity of air leaving AHU through exhaust air damper
V_{oa} velocity of air entering the AHU through outdoor air damper
V_{re} velocity of air through recirculation air duct
ρ air density
θ_{ex} fraction of fully open position of exhaust air damper
θ_{oa} fraction of fully open position of outdoor air damper
θ_{re} fraction of fully open position of recirculation air damper

REFERENCES

ASHRAE. 1989. *ASHRAE Handbook: Fundamentals*. Atlanta: American Society of Heating, Refrigerating, and Air-Conditioning Engineers, Inc.

ASHRAE. 1993a. *ASHRAE Handbook: Fundamentals*.

ASHRAE. 1993b. *Air-Conditioning Systems Design Manual*.

Datametrics, Inc. 1980. *Datametrics Instruction Manual*. Wilminton, Maine.

De Nevers, N. 1977. *Fluid Mechanics*. Reading, MA: Addison-Wesley.

Elovitz, D.M. 1995. Minimum Outside Air Control Methods for VAV Systems. *ASHRAE Transactions* (101)2: 613-618.

Janu, G.J., J.D. Wenger, and C.G. Nesler. 1995. Strategies for Outdoor Airflow Control from a Systems Perspective. *ASHRAE Transactions* (101)2: 631-643.

Kettler, J.P. 1995. Minimum Ventilation Control for VAV Systems: Fan Tracking vs. Workable Solutions. *ASHRAE Transactions* (101)2: 625-630.

Klein, S.A., and F.L. Alvardo.1994. *EES: Engineering Equation Solver*. Middleton, WI: F-Chart Software.

White, F.M. 1986. *Fluid Mechanics*, 2nd edition. New York: McGraw-Hill.